

## Monte Carlo method to calculate the central charge and critical exponents

Paul J. M. Bastiaansen\* and Hubert J. F. Knops

*Institute for Theoretical Physics, University of Nijmegen, P.O. Box 9010, 6500 GL Nijmegen, The Netherlands*

(Received 14 October 1997)

We present a finite size scaling technique to calculate the central charge and some critical exponents of two-dimensional critical models with a Monte Carlo simulation. We use systems with dimensions  $L \times M$ , and focus on the scaling behavior in  $M/L$ . The finite size scaling relation that we use is the universal expression for the stress tensor on the torus. The stress tensor is the operator that governs the anisotropy of the system, and stems from the theory of conformal invariance. We show that a lattice representation of the stress tensor can easily be constructed, such that its expectation value on the torus can be calculated in a Monte Carlo simulation. In doing so, we observe that the stress tensor turns out to be remarkably insensitive to critical slowing down. We show that the typical simulation time scales with the linear system dimension  $L$  roughly as  $L^4$ , and that this scaling holds for the ordinary Metropolis algorithm as well as for more sophisticated cluster algorithms, such that it is fruitless to invoke the latter. We test the method for the Ising model (with central charge  $c = \frac{1}{2}$ ), the Ashkin-Teller model ( $c = 1$ ), and the F model (also  $c = 1$ ). [S1063-651X(98)09103-X]

PACS number(s): 64.60.Ht, 05.70.Jk, 02.70.Fj, 02.70.Lq

### I. INTRODUCTION

There exist basically two methods to obtain numerical information on two-dimensional critical systems. In the transfer matrix method one calculates the largest eigenvalue of the transfer matrix and thus one finds the free energy of the system on a  $L \times \infty$  cylinder. From the theory of conformal invariance [1], one knows that this free energy is related to the central charge  $c$  as

$$f = f_\infty - \frac{\pi c}{6L^2}. \quad (1)$$

By introducing appropriate seams on the cylinder, that alter the cyclic boundary conditions, one also obtains some of the leading critical dimensions  $x$ . Here one uses the result from conformal invariance that the central charge  $\tilde{c}$  from a system with a seam is given by

$$\tilde{c} = c - 12x. \quad (2)$$

After the first paper [2] that used this technique, this method has become very popular [3,4].

The advantage of the method is the high numerical accuracy (in fact, machine precision) with which the free energy of a  $L \times \infty$  system can be determined. A distinct disadvantage is that it is limited to rather small values of  $L$ , since the required storage capacity and computer time increase exponentially with  $L$ . In some cases—depending on the system under scrutiny—the practical upper bound on  $L$  renders an accurate determination of the central charge impossible [5]. Notably, it implies that the method is limited to discrete spin systems.

These limitations are lifted but exchanged for a loss in numerical accuracy of the free energy in the Monte Carlo transfer matrix method [6,7]. A promising [8,9] method to

study the transfer matrix for discrete spin systems for large  $L$  is density matrix renormalization [10]. Recently, this method was shown to be able to calculate central charges [11].

The second method that was extensively used to obtain numerical information on two-dimensional critical systems is the standard [12] Monte Carlo (MC) method. It can be used for fairly large ( $L \times L$ ) system sizes, both for discrete and continuous spin systems. Critical exponents can be extracted from the finite size scaling behavior of the fluctuations in critical quantities like energy and order parameter.

However, a direct evaluation of the free energy is not possible in MC simulations. Therefore, to obtain the central charge from Eq. (1), one has to use a more elaborate MC method. Recently, Krech and Landau [13] proposed such a method, based on the work of Mon [14]. They tested their method on the  $q$ -state Potts model for  $q = 2, 3$ , and 4, and find an accurate agreement with the known results of the central charge of this model. Their method is based on the evaluation of an expectation value on a torus geometry  $L \times M$  of the form

$$\langle e^{-H_{\text{seam}}} \rangle. \quad (3)$$

Here  $H_{\text{seam}}$  is an Hamiltonian that introduces a seam in the direction of  $M$  over the torus. Hence this Hamiltonian is of the order of  $M$ , which has to be quite large. Such averages are notoriously hard to obtain in MC simulations.

Wang and Baker [15] used a method to evaluate the central charge that is not based on Eq. (1). Instead, they used an expression for the central charge due to Cardy [16], that involves the Fourier transform of the energy-energy correlation function. This expression contains the specific heat exponent  $\alpha$ , which has to be determined as well.

In this paper we want to extend this palette of existing numerical techniques by presenting a direct MC method to evaluate the central charge, which is based on the expectation value of a simple operator that can be defined for any model. This operator represents, in the scaling limit, the stress tensor  $T$ . The stress tensor is an operator that is con-

\*Electronic address: paulb@tvs.kun.nl

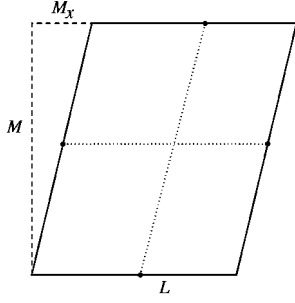


FIG. 1. The torus geometry on which the conformal field theory is defined. The dimensions of the torus are  $L \times M$ , the boundary conditions are such that the indicated points are identified: they are cyclic in the horizontal direction, and cyclic with a shift over  $M_x$  in the vertical direction.

nected with the anisotropy of the system; when one allows for anisotropy in critical models, critical points in the phase diagram become critical lines. The whole of such a critical line falls into the same universality class, and movements along the line are governed by a marginal operator, having its critical dimension  $x=2$ . This anisotropy operator is the stress tensor  $T$ , and can be defined for any critical model. It is, in the language of conformal invariance, the second descendant of the identity operator. The expectation value of  $T$  on a  $L \times M$  torus is known from conformal theory, and contains in particular the central charge  $c$ . By comparing our MC results, as a function of  $M/L$ , with this formula we obtain the central charge and the leading critical dimensions.

A difference between simulations on the stress tensor and on quantities like the energy is that the former are almost insensitive to critical slowing down. We explain this observation by showing how the typical simulation time scales with the system size in terms of the dynamic exponent  $z$ ; our conclusion is that it is fruitless to invoke sophisticated MC algorithms like that of Swendsen and Wang [17] that have a lower value of  $z$  than the standard Metropolis algorithm, because this would not influence the typical simulation time.

## II. CONFORMAL INVARIANCE OF CRITICAL FIELD THEORIES

Besides being invariant against a rescaling of the length parameters, critical models are believed to be conformally invariant as well: their large scale behavior is invariant against transformations that correspond locally to a rotation and a rescaling. Such transformations are called conformal transformations. From this symmetry, present at criticality, largely follows the structure of the Hilbert space, at least in the case of two-dimensional models. We will summarize some results that we need in the sequel; more details can be found in the review by Cardy [1].

In this section, we will be concerned with a system defined on a ‘‘skew’’ torus; its dimensions are  $L \times M$ , and boundary conditions are cyclic in the horizontal direction and cyclic after a shift over  $M_x$  in the vertical direction, as in Fig. 1. Denoting the transfer matrix of the system with  $\exp(-H)$ , where  $H$  is the Hamilton operator, its partition function on such a geometry is

$$Z = \sum_j \langle j | e^{-MH} e^{iM_x P} | j \rangle, \quad (4)$$

where the summation is over all configurations  $|j\rangle$  in a row. The states  $|j\rangle$  make up the Hilbert space on which the transfer matrix (or operator)  $\exp(-H)$  acts.  $P$  is the momentum operator, the generator of translations in the horizontal direction. The Hamilton operator  $H$  of the model is the generator of translations in the vertical direction, and commutes with  $P$ . When the transfer matrix is suitably defined, there exists an orthonormal basis of the Hilbert space, consisting of eigenstates of the Hamiltonian and of the momentum operator. From the theory of conformal invariance it follows that these eigenstates with their eigenvalues are closely related to the critical dimensions of the model.

There turns out to be a set of fundamental operators present in the theory, that are indicated as  $L_n$  and  $\bar{L}_n$  for  $n \in \mathbb{Z}$ . They satisfy the celebrated *Virasoro algebra*. The Hamiltonian  $H$  and the momentum operator  $P$  can be expressed in terms of  $L_0$  and  $\bar{L}_0$  as follows:

$$H = E_0 L + \frac{2\pi}{L} (L_0 + \bar{L}_0) - \frac{\pi c}{6L}, \quad (5)$$

$$P = \frac{2\pi}{L} (L_0 - \bar{L}_0). \quad (6)$$

Here  $c$  is the central charge of the model, and  $LE_0$  is the bulk ground state energy of the Hamiltonian, which we will not need and from now on consider subtracted from it. The eigenstates of the Hamiltonian and of the momentum operator are labeled as  $|\Delta + m, \bar{\Delta} + \bar{m}\rangle$ , with the relations

$$L_0 |\Delta + m, \bar{\Delta} + \bar{m}\rangle = (\Delta + m) |\Delta + m, \bar{\Delta} + \bar{m}\rangle, \quad (7)$$

$$\bar{L}_0 |\Delta + m, \bar{\Delta} + \bar{m}\rangle = (\bar{\Delta} + \bar{m}) |\Delta + m, \bar{\Delta} + \bar{m}\rangle. \quad (8)$$

Hence, with the bulk energy  $LE_0$  subtracted from the Hamiltonian,

$$\begin{aligned} H |\Delta + m, \bar{\Delta} + \bar{m}\rangle &= \frac{2\pi}{L} \left( \Delta + \bar{\Delta} + m + \bar{m} - \frac{c}{12} \right) |\Delta + m, \bar{\Delta} + \bar{m}\rangle, \end{aligned} \quad (9)$$

$$P |\Delta + m, \bar{\Delta} + \bar{m}\rangle = \frac{2\pi}{L} (\Delta - \bar{\Delta} + m - \bar{m}) |\Delta + m, \bar{\Delta} + \bar{m}\rangle. \quad (10)$$

The states  $|\Delta, \bar{\Delta}\rangle$  with  $m = \bar{m} = 0$  are called *primary states*, and the states with  $m$  and/or  $\bar{m}$  unequal to zero are their *conformal followers*. The values of  $\Delta$  and  $\bar{\Delta}$  are related to the critical dimensions  $x$  and spin indices  $l$  of the operators of the theory according to

$$x = \Delta + \bar{\Delta} + m + \bar{m}, \quad (11)$$

$$l = \Delta - \bar{\Delta} + m - \bar{m}. \quad (12)$$

The critical dimensions  $x$  are the complements with respect to the dimension  $d=2$  of the scaling indices  $y=d-x$ . These scaling indices are the eigenvalues of the renormalization flow equations in ordinary renormalization theory, and yield

expressions for the critical exponents. For example, in the Ising model there are two relevant fields: the thermal field which has  $y_t=1$ , and the magnetic field with  $y_m=\frac{15}{8}$ . The critical exponents are expressed in these indices as, e.g.,  $\alpha=(2y_t-2)/y_t=0$  for the specific heat exponent,  $\beta=(2-y_h)/y_t=\frac{1}{8}$  for the exponent of the order parameter, and  $\nu=1/y_t=1$  for the exponent governing the divergence of the correlation length.

The appearing values of  $\Delta$  and  $\bar{\Delta}$  from the primary states, together with their multiplicity (the level of their degeneracy) as well as the multiplicities of their conformal followers, determine the full structure of the Hilbert space. The values of the critical dimensions and their multiplicities are universal. This implies that the partition function (divided by its bulk value that results from  $E_0$ ) considered as a function of  $M/L$ , is universal in the scaling limit of  $L$  and  $M$  large.

From Eqs. (9) and (10) follows that the diagonal element of  $\exp(-MH)\exp(iM_xP)$  for the state  $|\Delta+m, \bar{\Delta}+\bar{m}\rangle$  is

$$Q^{-c/24}\bar{Q}^{-c/24}Q^{\Delta+m}\bar{Q}^{\bar{\Delta}+\bar{m}}, \quad (13)$$

with

$$Q = \exp\left(-\frac{2\pi M}{L} + \frac{2\pi i M_x}{L}\right), \quad (14)$$

and  $\bar{Q}$  the complex conjugate of  $Q$ . Summing over all diagonal elements yields the partition function of the model. Let us label the critical dimensions with  $j$ , then

$$Z/Z_{\text{bulk}} = Q^{-c/24}\bar{Q}^{-c/24}\sum_j N_j Q^{\Delta_j+m_j}\bar{Q}^{\bar{\Delta}_j+\bar{m}_j}. \quad (15)$$

This expression is called the *universal expression for the partition function*, and contains the central charge  $c$ , and the values of the critical dimensions  $\Delta_j+m_j$  and  $\bar{\Delta}_j+\bar{m}_j$  as well as their multiplicities  $N_j$ . Therefore, it contains the critical dimensions  $x_j$  and hence the critical exponents  $\alpha$ ,  $\beta$ , etc., although it does not give an interpretation of the dimensions  $x_j$  as belonging to thermal or magnetic fields.

In the limit  $M/L \rightarrow \infty$ , the universal expression for the partition function yields the well known finite size scaling relation for the central charge, used in transfer matrix calculations,

$$f(L) = f(\infty) - \frac{\pi c}{6L^2}, \quad (16)$$

where

$$f(L) = -\lim_{M/L \rightarrow \infty} \frac{1}{ML} \ln(Z). \quad (17)$$

The free energy, however, is not directly accessible in MC simulations. Consequently, apart from those mentioned in the introduction, there exist no MC results that yield the central charge of critical models. The stress tensor, however, is an operator that is closely related to the Hamilton operator, and it is this operator (or, rather its expression in terms of

spin variables) that actually *is* accessible in MC simulations, in contrast to the free energy. We will show this in the sequel.

Conformal invariance in critical field theories states that the action (or, in statistical mechanics terms, the classical interaction) is invariant against conformal transformations. The change in the action for nonconformal transformations is determined by the stress tensor  $T(\mathbf{r})$ ,

$$T(\mathbf{r}) = \begin{pmatrix} T_{xx}(\mathbf{r}) & T_{xy}(\mathbf{r}) \\ T_{yx}(\mathbf{r}) & T_{yy}(\mathbf{r}) \end{pmatrix}, \quad (18)$$

where  $T(\mathbf{r})$  is a symmetric, traceless tensor. Hence  $T_{xx}(\mathbf{r}) = -T_{yy}(\mathbf{r})$  and  $T_{xy}(\mathbf{r}) = T_{yx}(\mathbf{r})$ . Usually, one defines the independent components of  $T$  as

$$T(u,v) = \frac{1}{2}[T_{xx}(u,v) - iT_{xy}(u,v)], \quad (19a)$$

$$\bar{T}(u,v) = \frac{1}{2}[T_{xx}(u,v) + iT_{xy}(u,v)]. \quad (19b)$$

Here  $u$  and  $v$  are the position coordinates on the torus. The dimension  $(\Delta, \bar{\Delta})$  of  $T$  and  $\bar{T}$  are  $(2,0)$  and  $(0,2)$ , respectively. Hence their critical dimension  $x=2$  and their spin indices are  $l=\pm 2$ . So the stress tensor is a marginal operator. Its components  $T$  and  $\bar{T}$  can be expressed in terms of the fundamental Virasoro operators  $L_n$  and  $\bar{L}_n$  as follows:

$$T(u,v) = \left(\frac{2\pi}{L}\right)^2 \left(\frac{c}{24} - \sum_{n=-\infty}^{\infty} e^{-(2\pi i/L)un} e^{(2\pi/L)vn} L_n\right), \quad (20a)$$

$$\bar{T}(u,v) = \left(\frac{2\pi}{L}\right)^2 \left(\frac{c}{24} - \sum_{n=-\infty}^{\infty} e^{+(2\pi i/L)un} e^{(2\pi/L)vn} \bar{L}_n\right). \quad (20b)$$

This expression is valid on the torus geometry;  $u$  ( $v$ ) is the horizontal (vertical) position on the torus. The Virasoro operators  $L_n$  and  $\bar{L}_n$  with  $n \neq 0$  play the role of raising and lowering operators for the states  $|\Delta+m, \bar{\Delta}+\bar{m}\rangle$ . Because these states are orthonormal, only  $L_0$  and  $\bar{L}_0$  have nonvanishing contributions in the expression for the expectation value of  $T$ . From expression (20b) and the eigenvalue equations (8), the expression for the expectation value of the stress tensor can easily be calculated. The expectation value is

$$\langle T \rangle = \frac{1}{Z} \sum_j \langle \Delta_j+m_j, \bar{\Delta}_j+\bar{m}_j | T | \Delta_j+m_j, \bar{\Delta}_j+\bar{m}_j \rangle. \quad (21)$$

Substituting Eq. (20b) and the expression for the partition function (15) yields

$$\langle T \rangle = \left( \frac{2\pi}{L} \right)^2 \left( \frac{c}{24} \frac{\sum_j N_j (\Delta_j + m_j) Q^{-\Delta_j - m_j} \bar{Q}^{-\bar{\Delta}_j - \bar{m}_j}}{\sum_j N_j Q^{-\Delta_j - m_j} \bar{Q}^{-\bar{\Delta}_j - \bar{m}_j}} \right), \quad (22a)$$

$$\langle \bar{T} \rangle = \left( \frac{2\pi}{L} \right)^2 \left( \frac{c}{24} \frac{\sum_j N_j (\bar{\Delta}_j + \bar{m}_j) Q^{-\Delta_j - m_j} \bar{Q}^{-\bar{\Delta}_j - \bar{m}_j}}{\sum_j N_j Q^{-\Delta_j - m_j} \bar{Q}^{-\bar{\Delta}_j - \bar{m}_j}} \right). \quad (22b)$$

We will be mostly concerned with the diagonal elements  $T_{xx} = -T_{yy}$  of the stress tensor. The expression for  $T_{xx}$  is

$$\langle T_{xx} \rangle = \left( \frac{2\pi}{L} \right)^2 \times \left( \frac{c}{12} \frac{\sum_j N_j (\Delta_j + m_j + \bar{\Delta}_j + \bar{m}_j) Q^{-\Delta_j - m_j} \bar{Q}^{-\bar{\Delta}_j - \bar{m}_j}}{\sum_j N_j Q^{-\Delta_j - m_j} \bar{Q}^{-\bar{\Delta}_j - \bar{m}_j}} \right). \quad (23)$$

This expectation value can be written as the derivative of the free energy with respect to the aspect ratio  $M/L$ , as

$$\langle T_{xx} \rangle = -2\pi \frac{\partial f}{\partial \lambda} \quad \text{with} \quad \frac{M}{L} = e^\lambda. \quad (24)$$

Upon taking the derivative, the volume  $ML$  of the system is kept constant. Like magnetization and magnetic field, the ‘‘field’’  $\lambda = \ln(M/L)$  is the external field conjugate to the operator that is the stress tensor. Therefore,  $\langle T_{xx} \rangle$  couples to the anisotropy  $\lambda$  of the system, where the isotropic system has  $\lambda = 0$ .

### III. A LATTICE REPRESENTATION OF THE STRESS TENSOR

In conformal field theory, the stress tensor is an operator that is quite abstract. It is defined only after the lattice model has reached its continuum limit. For lattice models, however, the stress tensor can easily be defined as well. This lattice representation of the stress tensor must thus have the scaling behavior predicted by expression (23). Below we will illustrate the construction of the lattice representation of the stress tensor for the Ising model, but first we give a more general way to proceed.

#### A. Constructing the stress tensor

Construct, for a lattice model, an operator  $t(\mathbf{r})$  as an expression in the local, fluctuating field(s), such that (i)  $t(\mathbf{r})$  transforms as a second rank tensor [in particular,  $t(\mathbf{r})$  picks up a minus sign under a rotation over  $90^\circ$ ], and (ii)  $t(\mathbf{r})$  has the same symmetry as the interaction energy of the model under study. In general, this means that  $t(\mathbf{r})$  is invariant under global spin flips or spin rotations.

If one now expresses  $t(\mathbf{r})$  in terms of scaling operators it is clear that the operators that occur should all be tensors that change sign under rotations over  $\pi/2$ , i.e., they have  $l = \Delta - \bar{\Delta} = \pm 2, \pm 6, \dots$ . Since  $\Delta$  and  $\bar{\Delta}$  are always non-negative, it follows that the scaling dimension  $x$  of the appearing scaling operators all have  $x \geq 2$ . The marginal case, having  $x = 2$  and  $l = \pm 2$ , is in fact the stress tensor; all other operators in the expansion are irrelevant. To be more precise, in this general case, the operator  $t(\mathbf{r})$  couples to both independent components  $T_{xx}(\mathbf{r})$  and  $T_{xy}(\mathbf{r})$  of the stress tensor. As will become clear below, however,  $t(\mathbf{r})$  can easily be defined such that it couples to  $T_{xx}(\mathbf{r})$  only. In that case, one has

$$t(\mathbf{r}) = \alpha T_{xx}(\mathbf{r}) + \dots, \quad (25)$$

where the dots represent irrelevant operators. Requirement (ii) guarantees that  $t(\mathbf{r})$  and  $T_{xx}(\mathbf{r})$  share the same interaction symmetry, so that the coefficient  $\alpha$  does not vanish by symmetry. Constructing operators  $t(\mathbf{r})$  can, as we shall see, be done in several ways, but all choices yield expansion (25), albeit with different values of  $\alpha$ .

Having constructed the operator  $t(\mathbf{r})$  one can evaluate its average in a MC simulation on a geometry of  $L \times M$ , for several values of  $M/L$  and  $L$  large. The result should follow the universal expression for  $T_{xx}(\mathbf{r})$  as

$$\langle t(\mathbf{r}) \rangle = \alpha \langle T_{xx}(\mathbf{r}) \rangle + \mathcal{O}\left(\frac{1}{L^\omega}\right), \quad (26)$$

where the expression for  $\langle T_{xx}(\mathbf{r}) \rangle$  given in Eq. (23) is proportional to  $1/L^2$ , and dominates the second term that has  $\omega > 2$ . Hence we can fit the  $M/L$  dependence of the left hand side against Eq. (23), obtaining, in particular, the central charge  $c$ .

#### B. Stress tensor for the Ising model

We will illustrate the construction of the discrete stress tensor  $t(\mathbf{r})$  in the case of the Ising model. The starting point is the close connection between stress tensor and anisotropy. Let us therefore start with the anisotropic action  $\mathcal{A}$  of the ordinary, square lattice Ising model,

$$\mathcal{A} = - \sum_{ij} (J_x S_{i,j} S_{i+1,j} + J_y S_{i,j} S_{i,j+1}), \quad (27)$$

where the couplings  $(J_x, J_y)$  allow for anisotropy. The isotropic critical point is  $J_x = J_y = J_c = \frac{1}{2} \ln(1 + \sqrt{2})$ , but this point becomes a critical line when unequal values of  $J_x$  and  $J_y$  are allowed for.

The central notion here is that, in the scaling limit, anisotropy amounts to a rescaling of the length parameters  $x$  and  $y$  with a different scaling factor. Hence, in the scaling limit, the anisotropic model with  $(J_x, J_y)$  behaves as the isotropic model with rescaled length parameters  $x$  and  $y$ ,

$$x' = e^{-\lambda} x, \quad (28)$$

$$y' = e^{+\lambda} y. \quad (29)$$

The value of  $\lambda$  in this equation determines the values of  $J_x$  and  $J_y$ . In this way, Eq. (29) fixes the parametrization  $[J_x(\lambda), J_y(\lambda)]$  of the critical line with  $\lambda$ . The isotropic point has  $\lambda=0$  with  $J_x(0)=J_y(0)=J_c$ , and the parametrization obeys  $J_x(\lambda)=J_y(-\lambda)$ .

On a finite geometry  $L \times M$ , this anisotropic rescaling means that the volume  $ML$  of the system remains untouched, but that the aspect parameter  $M/L$  scales according to

$$\frac{M'}{L'} = e^{2\lambda} \frac{M}{L}. \quad (30)$$

In the scaling limit, therefore, the partition function with the anisotropic action of Eq. (27), which we call  $Z(\lambda, M/L)$  depending on  $\lambda$ , equals that of the isotropic Hamiltonian with a rescaled aspect ratio  $M'/L'$ ,

$$Z\left(\lambda, \frac{M}{L}\right) = Z\left(\lambda=0, e^{2\lambda} \frac{M}{L}\right). \quad (31)$$

A general movement in the phase diagram is performed by a scaling operator. A renormalization transformation is isotropic, which implies that there can be no renormalization flow along the critical line  $(J_x, J_y)$ . This implies that the scaling operator that governs the movement along this line must be invariant against a renormalization transformation, i.e., it is a marginal operator having its critical dimension  $x=2$ .

In the case of the Ising model, action (27) immediately shows which operator this must be. Write the action as a symmetric part plus a part that determines the anisotropy,

$$\mathcal{A} = \mathcal{A}_c - \sum_{ij} [J_x(\lambda) - J_c] S_{i,j} S_{i+1,j} + (J_y(\lambda) - J_c) S_{i,j} S_{i,j+1}, \quad (32)$$

where  $\mathcal{A}_c$  is the action at the isotropic critical point  $J_x=J_y=J_c$ . Expanding up to first order in  $\lambda$ , this expression can be written as

$$\mathcal{A} = \mathcal{A}_c + \lambda \sum_{ij} t_{xx}(i,j), \quad (33)$$

where  $t_{xx}(i,j)$  is the lattice representation of the stress tensor,

$$t_{xx}(i,j) = -J'_x(0) (S_{i,j} S_{i+1,j} - S_{i,j} S_{i,j+1}). \quad (34)$$

Here we used the symmetry property  $J_x(\lambda) = J_y(-\lambda)$ . The operator  $t_{xx}(i,j)$  governs the anisotropy of the system. This lattice representation of the stress tensor (34) for the Ising model was already known for a long time [18]; the value of  $J'_x(0) = \frac{1}{2}\sqrt{2}$ .

In fact, the operator in Eq. (34) is written as  $t_{xx}$  because it is one of the two components of the full stress tensor  $t_{\alpha\beta}(i,j)$ . This  $t_{\alpha\beta}(i,j)$  has the same properties as the field theoretical stress tensor: it is a second-rank, symmetric traceless tensor. The other component  $t_{xy}(i,j)$  can be written as

$$t_{xy}(i,j) = -J_{xy}(S_{i,j} S_{i+1,j+1} - S_{i,j} S_{i+1,j-1}), \quad (35)$$

with a certain prefactor  $J_{xy}$ , which will be different from  $J'_x(0)$ , because it couples next-nearest-neighbor spins instead of nearest neighbors. The off-diagonal elements of the discrete stress tensor couple to the anisotropy in the diagonal directions.

It is this operator  $t_{\alpha\beta}(\mathbf{r})$  that appeared in Sec. III A. It is constructed such that it behaves as a second-rank symmetric tensor with the same symmetry under global spin flips as the interaction energy itself. Of course, this version of  $t_{\alpha\beta}(i,j)$  is not the only possible one; it can also be defined with further neighbor interactions.

The precise connection between the discrete variant  $t(\mathbf{r})$  of the stress tensor and its field theoretical counterpart is obtained by taking the derivative of Eq. (31) with respect to  $\lambda$  at  $\lambda=0$ . Using Eq. (24), this yields

$$J'_x(0) \sum_{ij} \langle S_{i,j} S_{i+1,j} - S_{i,j} S_{i,j+1} \rangle = \frac{ML}{\pi} \langle T_{xx}(u,v) \rangle, \quad (36)$$

where  $\langle T_{xx}(u,v) \rangle$  is the expression [Eq. (23)] for the expectation value of the diagonal component of the stress tensor. Note that this expression is a universal function of central charge, critical dimensions, and their multiplicities. The value of  $J'_x(0)$ , however, is in general unknown, such that we will have to include it as a fit parameter.

Expression (36) combined with Eq. (23) yields the relation that is central to this work: it expresses the expectation value of the lattice representation of the stress tensor in terms of the universal quantities that we want to know. As we will use a rectangular geometry, without the shift in boundary conditions, we set  $M_x=0$  and obtain

$$\langle S_{i,j} S_{i+1,j} - S_{i,j} S_{i,j+1} \rangle = \alpha \left( \frac{2\pi}{L} \right)^2 \left( \frac{c}{12} - \frac{\sum_j N_j x_j \exp\left(-2\pi \frac{M}{L} x_j\right)}{\sum_j N_j \exp\left(-2\pi \frac{M}{L} x_j\right)} \right), \quad (37)$$

where  $1/\alpha = \pi J'_x(0)$ . See Fig. 2 for an example of the functional dependence. The prefactor  $\alpha$  is the same  $\alpha$  that appears in Eq. (25). The physical interpretation of it is given by the relation  $1/\alpha = \pi J'_x(0)$ ; it determines the ‘‘amount of anisotropy’’ that the system obtains, once the stress tensor is switched on. Note that  $\alpha$  is nonuniversal; it depends on the precise definition of the model, as well as on the definition of the stress tensor. The other quantities present in Eq. (37), however, are the central charge, the critical dimensions, and their multiplicities, and those are all universal. There is an infinite number of critical dimensions, but only a limited number of these is ‘‘small,’’ say, less than 2. For large enough values of the aspect ratio  $M/L$  only a limited number of critical dimensions have substantial contributions to Eq. (37); the contributions of the remaining dimensions then are in fact so small that they will fall in the noise of the MC data. Hence a fit of the expression against MC data must be feasible. Typically, we will take  $M/L \geq 1$ .

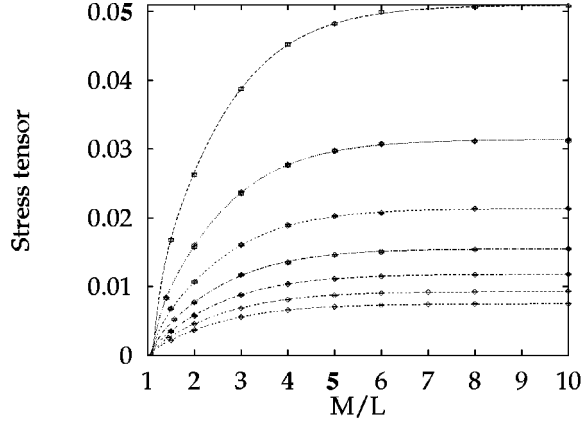


FIG. 2. The expectation values of stress tensor (1) for the Ising model, defined in Eq. (46b), as a function of the aspect parameter  $M/L$ . From high to low, the plots show the expectation values from system dimensions  $L$  running from 4 to 10. The lines are the result of the fit against Eq. (37) together with a correction to the scaling term (45). Note that, for each value of  $L$ , the stress tensor at  $M/L=1$  is zero by symmetry.

#### IV. FITTING THE MONTE CARLO RESULTS

Fitting the MC results against the universal expression for the stress tensor (37) requires a decent fit program, as the number of fit parameters is quite large, and requires some theoretical reflection on the model as well. We will deal with the use of the universal expression (37) and the corrections to scaling in different subsections.

##### A. Universal expression for the stress tensor

The number of critical dimensions  $x_j$  that appears in the universal expression (37) for the stress tensor is infinite, which clearly is an infeasible number of fit parameters. Most of the dimensions, however, are large. Their contribution to Eq. (37) goes as  $\exp(-2\pi x M/L)$ , so if we limit the calculations to values of the aspect ratio  $M/L$  that are not too small, most of the dimensions  $x_j$  have a vanishing contribution. Performing some preliminary MC simulations suggests a reasonable lower bound to  $M/L$ . Typically, we took  $M/L \geq 1$ . The upper bound on  $M/L$  is determined by the value of  $M/L$  where  $\langle t_{xx}(\mathbf{r}) \rangle$  reaches its asymptotic value. To determine a reasonable upper bound on  $M/L$ , the same preliminary simulations can be used. The asymptotic value of  $\langle t_{xx}(\mathbf{r}) \rangle$  is

$$\langle t_{xx}(\mathbf{r}) \rangle |_{M/L \rightarrow \infty} = \alpha \left( \frac{2\pi}{L} \right)^2 \frac{c}{12}. \quad (38)$$

This expression also shows why the asymptotic value itself is not sufficient for a determination of the central charge: it only gives an estimate of  $\alpha c$  instead of  $c$ .

Performing simulations to obtain the expectation value of the stress tensor between these bounds on  $M/L$  is in principle sufficient to extract the desired quantities by fitting the results against expression (37). Typically, we take three or four critical dimensions into account, the identity dimension  $x_0=0$ , present in any critical model, and two or three non-trivial ones  $x_j$ . For these dimensions, the multiplicities  $N_j$  must be specified in the expression as well.

A multiplicity is always integer, and when it is larger than 1, the corresponding critical dimension  $x$  is degenerate, and thus an additional symmetry is present in the model. Some theoretical reflection on the model often is sufficient to reveal such symmetries. Another possibility is to perform fits with different values of the multiplicities and to choose the set that gives the best fit.

The lowest appearing values of the dimensions  $x = \Delta + \bar{\Delta}$  correspond to primary fields. As noted in Sec. II, to each primary field belongs a tower of conformal followers or descendants, that have values of the critical dimensions that differ by an integer from that of the primary field; they are  $\Delta + m$  and  $\bar{\Delta} + \bar{m}$  with  $m, \bar{m} \in \mathbb{N}$ . The first descendant of a scalar primary field  $O(\mathbf{r})$  with dimensions  $(\Delta, \Delta)$  is  $\nabla O(\mathbf{r})$ , a vector field that has two components; one having  $(\Delta + 1, \Delta)$ , and the other having  $(\Delta, \Delta + 1)$ . To improve the fit, we will include this first descendant into Eq. (37). This inclusion introduces no new fit parameters; the value of its critical dimension is  $x+1$  when  $x$  is the critical dimension of the primary field, and this value appears twice. Hence the multiplicity of the first descendant is twice that of the corresponding primary field. Having fixed the multiplicities in expression (37), this leaves us with four or five free parameters: the prefactor  $\alpha$ , the central charge  $c$ , and two or three non-trivial dimensions  $x_j$ .

##### B. Corrections to scaling

The above analysis of the universal behavior of the stress tensor is valid in the scaling limit. The discrete version of the stress tensor  $t_{xx}(\mathbf{r})$ , however, is not a scaling field; as argued in Sec. III, it can in fact be written as expansion (25) in scaling fields, of which only the first term is the true stress tensor with its universal behavior. The fit to this expression is treated Sec. IV A, but for smaller system sizes other terms in the expansion become important. The scaling behavior of these terms in  $L$  goes as  $L^{-\omega}$  with  $\omega > 2$ .

To obtain accurate results, we should include at least one of these correction terms in the expression that we fit against our MC results. That means that we have to perform calculations for different values of the width  $L$  of the system in order to be able to extract the  $L^{-2}$  behavior of the true stress tensor.

In principle, we could proceed by performing simulations for a fixed value of  $M/L$  and increasing values of  $L$  and extract, by extrapolation, the part of  $\langle t_{xx}(\mathbf{r}) \rangle$  that scales as  $L^{-2}$ . This means that, for any value of  $M/L$ , we have to fit

$$\langle t_{xx}(\mathbf{r}) \rangle = \frac{a}{L^2} + \frac{b}{L^\omega}, \quad (39)$$

and have to use the values of  $a$  for each value of  $M/L$  to fit against expression (37). We can, however, do better.

To this end, write the first scaling operator on the dots in expansion (25) as  $O(\mathbf{r})$ ,

$$\langle t_{xx}(\mathbf{r}) \rangle = \alpha \langle T_{xx}(\mathbf{r}) \rangle + \langle O(\mathbf{r}) \rangle. \quad (40)$$

Now consider the general expression for the expectation value of an operator  $O(\mathbf{r})$  on a system with geometry  $L \times M$ ,

$$\langle O(\mathbf{r}) \rangle = \frac{1}{Z} \sum_j \langle j | e^{-MH} O(\mathbf{r}) | j \rangle, \quad (41)$$

with  $Z$  the partition function and  $H$  the Hamilton operator of Eq. (9). Using the basis  $|\Delta + m, \bar{\Delta} + \bar{m}\rangle$  of the Hilbert space yields

$$\langle O(\mathbf{r}) \rangle = \frac{\sum_j N_j a_j(L) e^{-2\pi(M/L)x_j}}{\sum_j N_j e^{-2\pi(M/L)x_j}}, \quad (42)$$

where we used Eq. (9). Here the parameters  $a_j(L)$  are the diagonal elements of the operator  $O(\mathbf{r})$  in the basis  $|\Delta + m, \bar{\Delta} + \bar{m}\rangle$  of the Hilbert space,

$$a_j(L) = \langle \Delta_j + m_j, \bar{\Delta}_j + \bar{m}_j | O(\mathbf{r}) | \Delta_j + m_j, \bar{\Delta}_j + \bar{m}_j \rangle. \quad (43)$$

As the basis functions  $|\Delta + m, \bar{\Delta} + \bar{m}\rangle$  depend only on  $L$  and not on  $M/L$ , the full  $M/L$  dependence of the expectation value  $\langle O(\mathbf{r}) \rangle$  is accounted for by the exponentials in Eq. (42). The amplitudes  $a_j(L)$  depend on  $L$  only. Taking only the leading correction into account, they can be written as

$$a_j(L) = \frac{a_j}{L^\omega}, \quad (44)$$

with the same value of  $\omega$  for each of the diagonal elements [1]. In our fit, we will only include the few most important critical dimensions  $x_j$ : the identity dimensions  $x_0 = 0$ , and the first two nontrivial ones. That means that including the expression for  $\langle O(\mathbf{r}) \rangle$  as a correction to scaling gives only four additional fit parameters: the correction exponent  $\omega$  and three amplitudes  $a_0$ ,  $a_1$ , and  $a_2$ .

In the other case, by naively extrapolating the behavior of  $\langle t_{xx}(\mathbf{r}) \rangle$  for large  $L$ , we have to include the two fit parameters  $\omega$  and  $b$  for each value of  $M/L$ . The above approach thus drastically reduces the number of fit parameters.

Still, in the complete analysis of the MC results, the number of fit parameters is quite large. Typically, we need four parameters from expression (37), which are the prefactor  $\alpha$ , the central charge  $c$ , and the two most relevant dimensions  $x_1$  and  $x_2$ . For the corrections to scaling, we use the expression following from Eqs. (42) and (44),

$$\langle O(\mathbf{r}) \rangle = \frac{1}{L^\omega} \frac{\sum_j N_j a_j e^{-2\pi(M/L)x_j}}{\sum_j N_j e^{-2\pi(M/L)x_j}}, \quad (45)$$

giving four additional parameters, which are  $\omega$ ,  $a_0$ ,  $a_1$ , and  $a_2$ .

In this way, we perform a combined fit of the MC results for all values of  $L$  and  $M/L$ , in one single fit using eight fit parameters. This is a large number, but the functional dependence of the formula, to be fitted for two variables simultaneously, is very restrictive. Especially for expression (37), the behavior in  $L$  is restricted to  $L^{-2}$ , and the values of the dimensions  $x_1$  and  $x_2$  appear as dimension as well as amplitude.

The number of critical dimensions  $x_j$  and the values of  $M/L$  that have to be included in the fit are a matter of trial and error. Sometimes it turned out to be necessary to delete some of the lowest values of  $M/L$  from the data set. Lower values of  $M/L$  clearly stabilize the fit, but on the other hand, including these values requires more critical dimensions from expression (37) to describe the full data set. We varied the lower bound on  $M/L$  and the number of critical dimensions, until the quality of the fit became high enough.

This procedure requires a fit program that yields, apart from the values of the fit parameters and their error bars, a parameter that indicates whether the fit can be trusted or not. Our case amounts to a two-dimensional fit (in  $L$  and  $M/L$ ) using eight or ten fit parameters. The program we used is based on routines from Ref. [19]. The parameter that indicates the quality of the fit is called the *goodness of fit*  $Q$ . The value of  $Q$  lies between 0 and 1, and is based on the  $\chi^2$  of the fitted data.  $Q$  gives the probability that the  $\chi^2$  of a certain data set exceeds that of the actual data set. A very low value of  $Q$  means that it is highly unlikely that the function used gives the correct theoretical description of the data. In our case this means that we either included values of  $M/L$  that are too small, or not enough critical dimensions  $x_j$ .

## V. COMPARISON WITH EXACTLY SOLVED MODELS

In order to test the method, we performed MC simulations on some models of which the scaling behavior on the torus is known exactly. We chose the Ising model (with central charge  $c = \frac{1}{2}$ ), the Ashkin-Teller model (with  $c = 1$ ), and the F model (also with  $c = 1$ ). There is a line in the phase diagram of the Ashkin-Teller model that can be mapped, by a duality transformation and a graphical representation [20], exactly on the F model. We chose to simulate the corresponding points in the Ashkin-Teller model and the F model. The results, however, differ, which is an illustration of the importance of boundary conditions in such simulations. The duality transformation alters the boundary conditions, giving rise to a different behavior of both models on a finite geometry.

In case of the Ising and Ashkin-Teller models, we performed MC simulations using the standard Metropolis algorithm. For the F model, we had to use a cluster algorithm as well (to be described below). We performed simulations on a system with geometry  $L \times M$  with varying values of  $L$  as well as of  $M/L$ . We sampled different versions of the stress tensor  $t_{xx}(\mathbf{r})$ , in order to obtain independent estimates of central charge and critical dimensions.

### A. Ising model

We carried out our simulations on the ordinary square lattice Ising model, with the action given in Eq. (27) at its isotropic critical point given by  $J_x = J_y = J_c = \frac{1}{2} \ln(1 + \sqrt{2})$ . The construction of the stress tensor is described in Sec. III. Actually, taking different versions of the discrete stress tensor  $t_{xx}(\mathbf{r})$  gives an independent check on the accuracy of the results. All different versions should couple to the true stress tensor  $T_{xx}(\mathbf{r})$ , albeit with different prefactors  $\alpha$ . We chose two versions of the discrete stress tensor, one defined with nearest-neighbor couplings and the other with next-next-nearest-neighbor couplings:

TABLE I. Monte Carlo results for the Ising model. Stress tensors (1) and (2) refer to the definition in Eq. (46b). Values of the prefactor  $\alpha$ , central charge  $c$ , and the first two critical dimensions  $x_1$  and  $x_2$  are given and compared with their exact values. Errors in the last digit are given in parentheses.  $\omega$  is the power of the  $1/L$  correction, and g.o.f. is the “goodness of fit.” In the case of stress tensor (1), the prefactor  $\alpha$  is known exactly [18].

	Stress tensor (1)	stress tensor (2)	Exact
$\alpha$	0.450 (2)	1.277 (3)	$\sqrt{2}/\pi=0.4501\dots^a$
$c$	0.500 (2)	0.498 (1)	1/2
$x_1$	0.1254 (6)	0.1256 (4)	1/8
$x_2$	1.0 (4)	1.1 (4)	1
$\omega$	4.3 (1)	4.29 (8)	
g.o.f.	0.83	0.97	

<sup>a</sup>Only for stress tensor (1).

$$(1) \quad \langle S_{i,j}S_{i+1,j} - S_{i,j}S_{i,j+1} \rangle, \quad (46a)$$

$$(2) \quad \langle S_{i,j}S_{i+2,j} - S_{i,j}S_{i,j+2} \rangle. \quad (46b)$$

Note that the stress tensor defined with next-nearest-neighbor couplings corresponds to the off-diagonal elements of the stress tensor; its expectation value on the geometry used is zero by symmetry. We took the system geometry  $L \times M$  with  $L$  varying from 4 to 10 and  $M/L$  varying from 1.5 to 10.

The resulting expectation values were fitted against expression (37) together with a correction to scaling term of Eq. (45). We took two nontrivial critical dimensions  $x_1$  and  $x_2$  into account, both with multiplicity 1. The data for stress tensor (1), together with the results of our fit, are plotted in Fig. 2 to obtain a feeling of the behavior of the stress tensor. The numerical results of the fit are summarized in Table I. Even for those small system sizes and correspondingly limited computer resources, accurate results are obtained.

### B. Ashkin-Teller model

A more severe test of the method is obtained by considering a model having dimensions lying closer to each other. The Ashkin-Teller model is a useful candidate for testing our method. It has in its phase diagram a critical line which can be mapped on the (exactly solved) six vertex model [20]. The universal partition sum of the Ashkin-Teller model on the torus is exactly known [21], so it can be compared with our MC results.

The Ashkin-Teller model has two Ising spins  $S$  and  $P$  with  $S, P \in \{+1, -1\}$  on each lattice site, that interact with an action

$$\mathcal{A} = - \sum_{\langle ij \rangle} J(S_i S_j + P_i P_j) + K S_i S_j P_i P_j, \quad (47)$$

where  $\langle ij \rangle$  denotes a summation over nearest-neighbor lattice sites. The critical line in the phase diagram that can be mapped on the six vertex model is parametrized by

$$\exp(2J) = \frac{1-W}{W}, \quad (48a)$$

$$\exp(2J+2K) = \frac{1+W}{1-W}. \quad (48b)$$

The weight  $W$  equals the Boltzmann weight of the four vertices in the six vertex model that carry a step. The other vertices are flat and have Boltzmann weight 1.

The critical line of Eq. (48b) is a line with central charge  $c=1$  and continuously varying exponents. By expressing the partition function of the Ashkin-Teller model in the scaling limit in terms of Coulomb gas partition functions, all critical exponents can be obtained. For this derivation, the reader is referred to Ref. [21]; we will only state the results.

Part of the exponents varies continuously along the critical line. Their value is expressed in terms of the renormalized value of the Gaussian coupling  $g$ , present in the Coulomb gas partition functions. The dimensions  $x$  of the primary fields are

$$x = \frac{e^2}{2g} + \frac{gm^2}{2} \quad \text{with } e, m \in \mathbb{Z}, \quad (49)$$

and  $g$  is the Gaussian coupling, given by

$$g = \frac{8}{\pi} \arcsin\left(\frac{1}{2W}\right). \quad (50)$$

The other dimensions are constant along the critical line. We chose, rather arbitrarily, the point  $W=0.8$  on the critical line for our simulations. At this point, the three most relevant dimensions are

$$x_1 = 0.125 \quad (\text{with multiplicity } 2), \quad (51a)$$

$$x_2 = 0.2908\dots \quad (\text{with multiplicity } 1), \quad (51b)$$

$$x_3 = 0.8596\dots \quad (\text{with multiplicity } 1). \quad (51c)$$

Typically, the multiplicity of the degenerate dimension  $x_1$  (which is constant along the critical line) can be guessed beforehand, though some theoretical reflection on the model is necessary. To this end, consider the expansion in scaling operators of  $S$  and  $P$ ,

$$S(\mathbf{r}) = \alpha_S p(\mathbf{r}) + \dots, \quad (52)$$

$$P(\mathbf{r}) = \alpha_P q(\mathbf{r}) + \dots, \quad (53)$$

where  $p(\mathbf{r})$  and  $q(\mathbf{r})$  are the leading (most relevant) scaling operators in the expansion. The manifest symmetry  $S \leftrightarrow P$  of action (47) implies that

$$\alpha_S^2 \langle p(\mathbf{r}_1) p(\mathbf{r}_2) \rangle = \alpha_P^2 \langle q(\mathbf{r}_1) q(\mathbf{r}_2) \rangle. \quad (54)$$

Hence it follows that  $p(\mathbf{r})$  and  $q(\mathbf{r})$  share the same critical dimensions  $x$ . On the other hand, spin reversal symmetry  $S \rightarrow -S$  implies that

$$\langle S(\mathbf{r}_1) P(\mathbf{r}_2) \rangle = 0, \quad (55)$$

which implies that the dominant term for  $|\mathbf{r}_1 - \mathbf{r}_2|$  large in this expression must vanish as well. Hence

$$\alpha_S \alpha_P \langle p(\mathbf{r}_1) q(\mathbf{r}_2) \rangle = 0. \quad (56)$$



TABLE II. Monte Carlo results for the Ashkin-Teller model, corresponding to the six vertex model with Boltzmann weight  $W=0.8$ . The stress tensors (1)–(4) are defined in Eq. (57d). For notation, see Table I.

	Stress tensor (1)	Stress tensor (2)	Stress tensor (3)	Stress tensor (4)	Exact
$\alpha$	0.36 (2)	0.78 (3)	0.23 (1)	0.65 (2)	
$c$	0.97 (6)	0.99 (3)	0.96 (4)	0.96 (3)	1
$x_1$	0.128 (3)	0.130 (2)	0.128 (3)	0.128 (2)	0.125
$x_2$	0.33 (8)	0.34 (5)	0.34 (6)	0.35 (4)	0.2908...
$x_3$	0.9 (4)	0.8 (1)	0.9 (3)	0.9 (2)	0.8596...
$\omega$	3.8 (2)	4.1 (1)	4.0 (2)	4.2 (1)	
g.o.f.	0.80	0.016	0.76	0.065	

This ensures that  $p(\mathbf{r})$  and  $q(\mathbf{r})$  are *different* scaling operators sharing the same critical dimension  $x$ . Therefore this magnetic critical dimension  $x$  must have multiplicity 2. Note that the second argument does not apply for energylike operators like  $S_{i,j}S_{i+1,j}$ , such that the energy scaling field will be nondegenerate.

We performed MC simulations using the standard Metropolis algorithm, again on the system with geometry  $L \times M$ , with  $L$  varying from 5 to 12 and  $M/L$  varying from 1.5 to 10. We sampled four different versions of the stress tensor  $t_{xx}(\mathbf{r})$ :

$$(1) \quad \langle S_{i,j}S_{i+1,j} + P_{i,j}P_{i+1,j} - S_{i,j}S_{i,j+1} - P_{i,j}P_{i,j+1} \rangle, \quad (57a)$$

$$(2) \quad \langle S_{i,j}S_{i+2,j} + P_{i,j}P_{i+2,j} - S_{i,j}S_{i,j+2} - P_{i,j}P_{i,j+2} \rangle, \quad (57b)$$

$$(3) \quad \langle S_{i,j}P_{i,j}S_{i+1,j}P_{i+1,j} - S_{i,j}P_{i,j}S_{i,j+1}P_{i,j+1} \rangle, \quad (57c)$$

$$(4) \quad \langle S_{i,j}P_{i,j}S_{i+2,j}P_{i+2,j} - S_{i,j}P_{i,j}S_{i,j+2}P_{i,j+2} \rangle. \quad (57d)$$

Stress tensors (1) and (2) are defined such that the symmetry between  $S$  and  $P$  spins is incorporated.

It turns out that in this case three nontrivial dimensions have to be included in the fit. This brings the total number of fit parameters to no less than 10. Still, relatively good results are obtained; they are summarized in Table II.

### C. F model

A nice illustration of the importance of boundary conditions is obtained when a dual version of the Ashkin-Teller model is considered. As stated, the critical line of the Ashkin-Teller model can be mapped exactly onto the F model, using a duality transformation and a graphical representation [20]. On a finite system, however, this mapping affects the boundary conditions, such that both models with periodic boundary conditions will have a different behavior on the torus.

The model we chose to consider in fact is an intermediate model between the F model and the Ashkin-Teller model, and is obtained from the latter by applying a duality transformation on one of the spins  $S$  or  $P$  only. In this way, we obtain two coupled Ising models, defined on two interpenetrating sublattices. Both Ising models are equal; they interact via a nearest-neighbor coupling such that a broken Ising

bond carries a Boltzmann weight  $W$ , where the weight  $W$  is the same as the  $W$  in Eq. (48b) of the Ashkin-Teller model. The coupling between the Ising models only exists in the restriction that two broken Ising bonds are not allowed to cross each other. An elementary square of the lattice contains two spins of both sublattices; diagonally opposed spins belong to the same sublattice. The restriction is that at most one of the bonds over the elementary square may be broken.

The resulting model can easily be mapped on the F model, seen as a body centered solid on solid (BCSOS) height model [22]. To this end, the Ising-Bloch walls are identified with the steps, carried by the first four vertices of the F model. To become steps, walls have to be equipped with an arrow; the steps have to be identified as a step up or a step down. This arrow assignment is simply such that two adjacent Ising-Bloch walls carry antiparallel arrows if they belong to the same sublattice, and carry parallel arrows if they belong to different sublattices.

In this way, a configuration of the two Ising models is mapped onto a configuration of the F model, and vice versa. There is, however, a difference in boundary conditions on the torus. If we consider the F model on a finite geometry as a height model, we have to allow for defects at the boundary. The smallest defect in the F model is a defect of two unit heights, which corresponds to two steps running over the system. The corresponding Ising configuration however, would have one Ising-Bloch wall running over the system for each sublattice, which is not allowed when the two Ising models have periodic boundary conditions. Hence for the F model the allowed defects at the boundary are height differences multiples of 2, whereas in the formulation of the Ising models, the height differences at the boundary are multiples of 4.

Related to these defects is a complication that arises, when one naively tries to simulate this version of the F model using a single-spin Metropolis algorithm. As the updates in such an algorithm are always local, it cannot generate configurations with defects around the torus. The algorithm is able to generate islands of flipped spins, but such an island never can cross an Ising-Bloch wall of the other sublattice. This implies that the algorithm is nonergodic; the part of phase space it reaches is restricted to that part that has the same defects at the boundary as the initial configuration.

That does not mean that the results of the simulation make no sense. The model that results when using only the Metropolis algorithm is a true height model, such that on the boundaries no defects are allowed at all. This model renormalizes to the Gaussian model. The universal form of its

TABLE III. Monte Carlo results for the F model with Boltzmann weight  $W=0.8$ . Two different stress tensors are used for the calculation of the central charge and critical dimensions. They are defined in Eq. (58b). For notation, see Table I.

	Stress tensor (1)	Stress tensor (2)	Exact
$\alpha$	0.83 (6)	1.32 (7)	
$c$	1.06 (7)	1.03 (6)	1
$x_1$	0.291 (6)	0.289 (5)	0.2908...
$x_2$	0.7 (1)	0.65 (9)	0.8596...
$\omega$	3.2 (2)	2.8 (1)	
g.o.f.	0.28	0.27	

partition function is known [23], but behaves somewhat anomalously because it has a continuous spectrum of critical dimensions, that result in an integral instead of a sum in Eq. (37). The universal partition sum of the Gaussian model is the result of this integral. Inclusion of its form in our fit for this model indeed yields the correct result.

The difficulty in boundary conditions, however, can easily be overcome using a cluster algorithm, that allows for non-local updates of the configurations. In our simulations, we used a standard Metropolis algorithm for thermal equilibration, combined with a cluster algorithm [17,24] that is able to generate defects, in order to make sure that the whole phase space can be reached. We performed simulations on the model with  $L$  varying from 6 to 18 and  $M/L$  from 2 to 5. It turned out in this case the stress tensor reaches its asymptotic value already for  $M/L \approx 5$ .

We sampled two possible versions of the stress tensor,

$$(1) \quad \langle S_{i,j} S_{i+2,j} - S_{i,j} S_{i,j+2} \rangle, \quad (58a)$$

$$(2) \quad \langle S_{i,j} S_{i+3,j+1} - S_{i,j} S_{i-1,j+3} \rangle, \quad (58b)$$

where we took into account that energylike spin products always must couple spins of the same sublattice. The most simple version of the stress tensor couples nearest-neighbor spins of each sublattice, but its expectation value on the system geometries that we considered is zero by symmetry. Stress tensor (2) is, regarding its definition, a mix of  $t_{xx}(\mathbf{r})$  and  $t_{xy}(\mathbf{r})$ , but this is no problem since, on the used geometry, any  $t_{xy}(\mathbf{r})$  is zero.

The fact that this model is a height model ensures that there are basically two types of operators, spin wave and vortex operators, with dimensions given in Eq. (49), that both are doubly degenerate. (cf. Ref. [25] for further discussion.) Hence the lowest critical dimensions have multiplicity 2. We fitted the resulting expectation values of the different stress tensors, using two non-trivial critical dimensions. The results are summarized in Table III.

It is noteworthy that the prefactor  $\alpha$  in the definition of the stress tensor is independent of the boundary conditions. Our fit on the simulation that only used the Metropolis algorithm (described above) yielded the same prefactors as those in Table III. That means that expansion (25) of the discrete stress tensor in terms of scaling fields only depends on local properties.

It turned out that including values of  $M/L$  smaller than 2 destroyed the quality of the fit, yielding a far too low value of the goodness of fit. The reason probably is that there are much more dimensions  $x_j$  present that are quite small and that start to become important for values of  $M/L$  smaller than 2. This can be seen from the value of  $x_2$  that follows from the fit; it is significantly lower than the exact value of the second dimension. Apparently, in the fit program  $x_2$  plays the role of an ‘‘effective’’ dimension, incorporating the values of several dimensions in one. This casts doubt on the validity of the highest dimension that is given by the fit program, but is seen not to affect the values of the central charge  $c$  and the most relevant dimension  $x_1$ .

## VI. SIMULATION TIMES AND AUTOCORRELATIONS

MC calculations of a marginal operator like the stress tensor typically encounter additional difficulties as compared to observables like energy and magnetization. The latter quantities have a relative error in MC simulations that does not scale with the system size, whereas this is not the case for an operator like the stress tensor; its relative error increases with the system size.

This can be seen as follows: consider an operator  $O(\mathbf{r})$  of which we want to calculate its expectation value. Its scaling behavior will be dictated by a critical dimension  $x$ ,

$$\frac{1}{L^2} \sum_{\mathbf{r}} \langle O(\mathbf{r}) \rangle \sim L^{-x}, \quad (59)$$

where  $L$  is the linear system size. The error  $\Delta_{O(\mathbf{r})}$  in the average value is related to the number of samples  $N$  in the MC simulation and to the second moment of its distribution,

$$\Delta_{O(\mathbf{r})}^2 = \frac{1}{N} \frac{1}{L^4} \sum_{\mathbf{r}, \mathbf{r}'} \langle O(\mathbf{r}) O(\mathbf{r}') \rangle - \langle O(\mathbf{r}) \rangle \langle O(\mathbf{r}') \rangle. \quad (60)$$

Note that  $N$  stands for the number of statistically *independent* MC samples. The dependence on  $L$  of the simulation time to reach independent samples will be discussed below.

Typically, the double summation in the last expression has two contributions; a short range contribution and a long range contribution. The short range contribution, say within a region with radius  $R$ , follows

$$\sum_{|\mathbf{r}| < R} \langle O(\mathbf{r}) O(0) \rangle - \langle O(\mathbf{r}) \rangle \langle O(0) \rangle \rightarrow \text{const} \quad (61)$$

for  $L$  large. The constant is roughly proportional to the radius  $R$  when it is not too large. The long range contribution, on the other hand, is dominated by the critical dimension  $x$  as

$$\sum_{|\mathbf{r}| > R} \langle O(\mathbf{r}) O(0) \rangle - \langle O(\mathbf{r}) \rangle \langle O(0) \rangle \sim L^{2-2x}. \quad (62)$$

Now there are two cases. If the dimension  $x \leq 1$  the long range contribution dominates Eq. (60), and the relative error in  $\langle O(\mathbf{r}) \rangle$  scales according to

$$\frac{\Delta_{O(\mathbf{r})}}{\langle O(\mathbf{r}) \rangle} \sim \frac{1}{\sqrt{N}}. \quad (63)$$

It is inversely proportional to the square root of the number of MC samples, but does not scale with the system size  $L$ . This is the usual case for, e.g., magnetization and energy in the Ising model. In case  $x > 1$ , however, the short range contribution dominates the error for large  $L$ , which implies that the relative error in  $\langle O(\mathbf{r}) \rangle$  scales according to

$$\frac{\Delta_{O(\mathbf{r})}}{\langle O(\mathbf{r}) \rangle} \sim \frac{1}{\sqrt{N}} L^{x-1}. \quad (64)$$

We will want to obtain the same relative error for all different linear system dimensions  $L$  in our MC simulations. For observables having  $x \leq 1$  this requires the same number of MC samples for all  $L$ . For  $x > 1$ , however, Eq. (64) dictates that  $N \sim L^{2x-2}$ . In case of the stress tensor, having  $x = 2$ , the number of MC samples should thus be proportional to  $L^2$ .

At first sight, it seems that this fact makes it difficult to reach large system sizes, as the simulation time is directly proportional to the number of required MC samples. This, however, is only partly true. The other parameter which determines the simulation time is the time it takes to generate statistically independent configurations. Critical systems are known to suffer from critical slowing down. If one uses the standard Metropolis algorithm, the typical time  $\tau$  it takes to generate statistically independent configurations increases with the system size as a power law.

Unexpectedly, it turns out that the stress tensor is remarkably insensitive to critical slowing down. This can be judged from its autocorrelation function. Let us define a MC cycle as one attempted update per spin. The autocorrelation function of a certain observable  $O$  is defined as

$$g(t) = \frac{\langle O_{t_0} O_{t_0+t} \rangle - \langle O_{t_0} \rangle^2}{\langle O_{t_0}^2 \rangle - \langle O_{t_0} \rangle^2}. \quad (65)$$

The operator  $O$  is, as usual, defined as  $\sum_{\mathbf{r}} O(\mathbf{r})$ . Here  $O_t$  denotes the value of  $O$  after  $t$  time steps, where a time step is one cycle, i.e., one attempted update per spin. The autocorrelation function  $g(t)$  is normalized such that  $g(0) = 1$ . In practical situations, the number of MC cycles  $t$  between two consecutive MC samples has to be such that  $g(t)$  is (almost) zero.

The observation that the stress tensor does not suffer very much from critical slowing down follows from Fig. 3. Here we plotted the autocorrelation functions  $g(t)$  for the energy and the stress tensor, in the case of the Ising model at its critical point, for several different system dimensions. For a number of cycles  $t$  not too small, the autocorrelation function of the energy shows a straight line in the log-normal plot, meaning that its behavior is exponential in  $t$ . Indeed, the behavior of the autocorrelation functions for nearly critical systems is given by

$$g(t) \sim \exp(-t/\tau) \quad \text{for } t \text{ large}, \quad (66)$$

where  $\tau$  is the autocorrelation time. The dynamic scaling hypothesis states that the time scale  $\tau$  of a dynamical system is connected with the length scale, which is the correlation length  $\xi$ , and that this connection is described by a universal dynamic exponent  $z$ ,

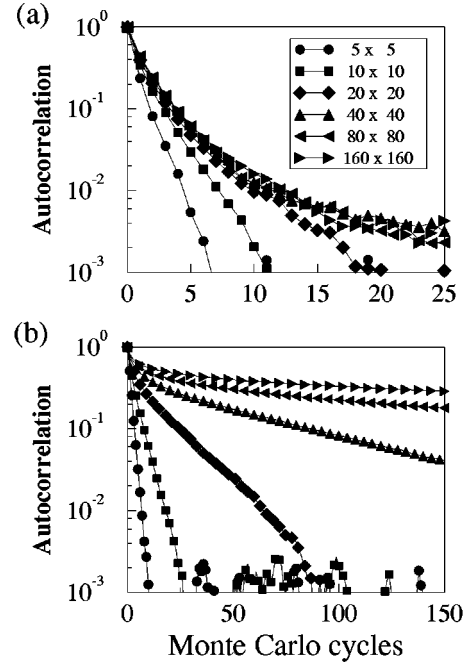


FIG. 3. Plots of the autocorrelation function  $g(t)$  of Eq. (65), where  $t$  is the number of Monte Carlo cycles. Calculations are performed using the Metropolis algorithm for the Ising model at its critical point. System dimensions are indicated in the figure. (a) Autocorrelation function of the stress tensor. (b) Autocorrelation function of the energy. Note the difference in scale of the  $x$  axes of the plots.

$$\tau \sim \xi^z. \quad (67)$$

The exponent  $z$  is believed to be connected to the dynamics of the system (in our case, by the Metropolis algorithm) and to be the same for all observables. For finite systems at their critical point, the correlation length  $\xi$  is bounded by the system dimension  $L$ , such that

$$\tau(L) \sim L^z. \quad (68)$$

We extracted the values of  $\tau(L)$ , following from the autocorrelation function of the energy in Fig. 3, by fitting the autocorrelation functions to Eq. (66). For this, we removed the first data points, up to the point where the plot begins to show a straight line. The values of  $\tau(L)$  were fitted to Eq. (68), yielding a value for  $z$  of roughly 2. The quoted value in the literature [26] is  $z \approx 2.17$ , which is consistent with our findings.

The autocorrelation behavior of the stress tensor, however, is dramatically different from that of the energy. Note the difference in scale of the  $t$  axes in Fig. 3. The autocorrelation function of the stress tensor drops so sharply that the exponential behavior can hardly, if at all, be seen. There is almost no sign of critical slowing down; the autocorrelation functions even seem to converge for larger and larger systems. Even for systems as large as  $180 \times 180$  spins the autocorrelation function behaves not significantly different from smaller system sizes.

These findings can be explained as follows. The dynamic scaling hypothesis in its general form considers the combined spatial and time correlation function  $G(\mathbf{r}, t)$ , defined as

$$G(\mathbf{r}, t) = \langle O(\mathbf{r}_0, t_0) O(\mathbf{r}_0 + \mathbf{r}, t_0 + t) \rangle - \langle O(\mathbf{r}_0, t_0) \rangle^2 \quad (69)$$

for a certain operator  $O(\mathbf{r}, t)$ . Here the dynamics of the system is explicitly taken into account by the time dependence of the operator. The dynamic scaling hypothesis states that

$$G(\mathbf{r}, t) = b^{-2x} G(b^{-1}\mathbf{r}, b^{-z}t), \quad (70)$$

where  $x$  is the critical dimension of the operator  $O(\mathbf{r}, t)$ . In terms of this correlation function, the autocorrelation function  $g(t)$  of Eq. (65) can be expressed as

$$g(t) = \frac{\int_0^L d^2\mathbf{r} G(\mathbf{r}, t)}{\int_0^L d^2\mathbf{r} G(\mathbf{r}, 0)}. \quad (71)$$

The integral is over the finite volume  $L^2$ . The dynamic scaling hypothesis (70) will be valid provided that the appearing lengths are smaller than the correlation length  $\xi$ , and the times are smaller than the autocorrelation time  $\tau$ , given by  $\tau \sim \xi^z$ . For finite systems,  $\xi \sim L$ . In that case, Eq. (70) can be rephrased to

$$G(\mathbf{r}, t) = t^{-2x/z} G(t^{-1/z}\mathbf{r}, 1), \quad (72)$$

which yields the  $L$  and  $t$  dependences in the scaling limit of Eq. (71). Using Eq. (70), the numerator is

$$t^{(2-2x)/z} \int_0^{t^{-1/z}L} d^2\mathbf{r} G(\mathbf{r}, 1), \quad (73)$$

and  $G(\mathbf{r}, 1)$  must follow the usual spatial behavior  $|\mathbf{r}|^{-2x}$ . Now the scaling behavior of the integral depends on whether it converges or diverges for large  $L$ . Making this distinction, the scaling behavior of Eq. (71) is

$$g(t) \sim \text{const} \quad \text{for } x < 1, \quad (74)$$

$$g(t) \sim t^{(2-2x)/z} \quad \text{for } x \geq 1. \quad (75)$$

This explains our MC results: both cases indicate that  $g(t)$  must become independent of  $L$  in the scaling limit, i.e., for large  $L$ . The case of the energy, having  $x = 1$ , states that  $g(t)$  must converge to a value independent of  $t$ , whereas the case of the stress tensor implies that  $g(t)$  becomes a true power law in  $t$ . This behavior indeed can be seen in Fig. 4, where, for the stress tensor and for the energy, the values of  $g(t)$  are plotted as a function of system size  $L$  for several values of  $t$ . The plot for the energy indicates that  $g(t)$  converges to 1, whereas the asymptote of  $g(t)$  for the stress tensor is seen to depend on  $t$ .

The above analysis also enables us to determine the scaling of the typical simulation time of a MC simulation with the system size  $L$ . This scaling will depend on the MC algorithm (i.e., on  $z$ ) and on the observable we want to know. Starting point is that we will want to obtain the same relative error in the average value  $\langle O(\mathbf{r}) \rangle$  for each system dimension  $L$ . The error  $\Delta_{O(\mathbf{r})}$  in the average is proportional to the second moment of the correlation function,

$$\Delta_{O(\mathbf{r})}^2 = \frac{1}{N} \frac{1}{L^2} \int_0^{L^z} dt \int_0^L d^2\mathbf{r} G(\mathbf{r}, t). \quad (76)$$

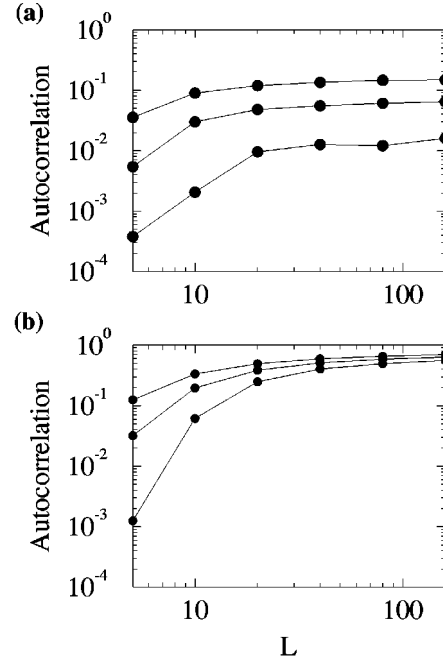


FIG. 4. Plots of the autocorrelation function  $g(t)$  of Eq. (65) vs the system size  $L$ . From high to low, the plots amount to  $t=3, 5$ , and  $10$ . (a)  $g(t)$  for the stress tensor. (b)  $g(t)$  for the energy. The plots show that for the energy,  $g(t)$  converges to a value independent of  $t$ , which must be 1. For the stress tensor, however,  $g(t)$  converges to a value that does depend on  $t$ .

Here  $N$  is the total number of MC cycles, which is supposed to be much larger than the autocorrelation time  $L^z$ . Using, as above, Eq. (70) and the distinction between converging and diverging integrals with  $L$ , we obtain

$$\Delta_{O(\mathbf{r})}^2 \sim \frac{1}{N} L^{z-2x} \quad \text{for } x < 1 + \frac{1}{2}z, \quad (77)$$

$$\Delta_{O(\mathbf{r})}^2 \sim \frac{1}{N} L^{-2} \quad \text{for } x \geq 1 + \frac{1}{2}z. \quad (78)$$

The relative error is obtained by dividing these values by  $\langle O(\mathbf{r}) \rangle$ , which scales as  $L^{-x}$ . The typical number of MC cycles  $N$  is obtained by demanding it to be such that the same relative error is obtained for all  $L$ . This yields

$$N \sim L^z \quad \text{for } z > 2x - 2, \quad (79)$$

$$N \sim L^{2x-2} \quad \text{for } z \leq 2x - 2. \quad (80)$$

This implies that, for a relevant operator, like the energy in the Ising model, faster convergence is obtained by a MC algorithm that has a lower value of the dynamic exponent  $z$ , and lowering this value is precisely the point of the cluster algorithm [17]. However, the case of the stress tensor,  $x = 2$ , represents a border case, because for the Metropolis algorithm  $z$  is only slightly larger than 2. As a result, it is fruitless to invoke the more sophisticated cluster algorithms for simulations on the stress tensor.

Note that the actual simulation *time* is, in the case of a Metropolis algorithm, proportional to  $L^2 N$ , because the time needed for a single MC cycle is simply proportional to the number of spins. An important consequence of the above is

that the typical simulation time for the stress tensor is roughly proportional to  $L^4$ . This contrasts with the computer time needed for transfer matrix calculations, which is exponential in  $L$ .

Hence, in principle much larger system sizes can be reached with our MC method than in the transfer matrix method, to calculate the central charge. This is a promising conclusion for systems of which the value of the central charge up to now is an open question [27,5].

## VII. SUMMARY AND DISCUSSION

In this paper, we proposed a Monte Carlo technique for the calculation of the central charge, and some critical dimensions of two-dimensional critical models. The technique is based on the universal behavior of the stress tensor, an operator that plays an important role in the theory of conformal invariance, but of which a lattice representation can easily be found as well. The rough data, following from the Monte Carlo simulation, require a decent fit program to extract the central charge and critical dimensions. By comparing our Monte Carlo analysis for three different models with their exact results, we showed that the method works. We explained why, on one hand, simulations on the stress tensor are difficult because its expectation value is equipped with larger error bars than usual. On the other hand, it turns out that the simulations are much easier than usual because the stress tensor shows to be remarkably insensitive to critical slowing down. The latter observation notably ensures that the typical simulation time of our method scales with the system size  $L$  roughly as  $L^4$ , in contrast with transfer matrix

calculations, which scale exponentially as  $n^L$ , where  $n$  is the number of different spin states.

Hence much larger system sizes can be reached with our proposed method than with transfer matrix calculations, at least in principle. For that reason, we expect the merits of our method as compared with transfer matrix calculations to lie mainly in simulations on models with a large number of spin states  $n$ , especially when these states become continuous, as, e.g., in the XY-Ising model.

It is not immediately clear what the advantages (if any) of our method are over the MC methods of Krech and Landau [13] or Wang and Baker [15], mentioned in Sec. I. With these latter methods, the observables to be averaged in the MC simulation are more difficult than in our method. To obtain accurate results, Krech and Landau had to use the Wolff algorithm [24] and the optimized multiple histogram analysis of Ferrenberg and Swendsen [28], together with large computer power. The results in this paper were obtained using standard Metropolis without histogram analysis, on a simple workstation with moderate simulation times, but are admittedly less accurate. Wang and Baker used a relation for the central charge that contains the specific heat exponent  $\alpha$  as an unknown, and had to sample a region of the phase diagram in the neighborhood of the critical point. The strength of our method as compared to these other techniques remains to be seen.

## ACKNOWLEDGMENTS

It is a pleasure to thank Henk Blöte for discussions on dynamical systems, and Michael Krech for drawing our attention to Ref. [13].

- 
- [1] See, e.g., J. L. Cardy in *Phase Transitions and Critical Phenomena*, edited by C. Domb and J. Lebowitz (Academic, London, 1987), Vol. II.
  - [2] H. W. J. Blöte, J. L. Cardy, and M. P. Nightingale, *Phys. Rev. Lett.* **56**, 742 (1986).
  - [3] G. von Gehlen and V. Rittenberg, *J. Phys. A* **19**, L625 (1986).
  - [4] K. Rommelse and M. den Nijs, *Phys. Rev. Lett.* **59**, 2578 (1986); *Phys. Rev. B* **40**, 4709 (1989).
  - [5] P. J. M. Bastiaansen and H. J. F. Knops, *Phys. Rev. B* **53**, 126 (1996).
  - [6] M. P. Nightingale and H. W. J. Blöte, *Phys. Rev. Lett.* **60**, 1562 (1988).
  - [7] J. M. Thijssen and H. J. F. Knops, *Phys. Rev. B* **42**, 2438 (1990).
  - [8] T. Nishino, *J. Phys. Soc. Jpn.* **64**, 3598 (1995).
  - [9] E. Carlon and A. Drzewinski, *Phys. Rev. Lett.* **79**, 1591 (1997).
  - [10] S. R. White, *Phys. Rev. B* **48**, 10 345 (1993).
  - [11] E. Carlon and F. Iglói, *Phys. Rev. B* (to be published).
  - [12] See, e.g., *Applications of the Monte Carlo Method in Statistical Physics*, edited by K. Binder (Springer-Verlag, Berlin, 1984).
  - [13] M. Krech and D. P. Landau, *Phys. Rev. E* **53**, 4414 (1996).
  - [14] K. K. Mon, *Phys. Rev. Lett.* **54**, 2671 (1985); *Phys. Rev. B* **35**, 3560 (1987).
  - [15] X. Wang and G. A. Baker, Jr., *J. Stat. Phys.* **69**, 1069 (1992).
  - [16] J. L. Cardy, *Phys. Rev. Lett.* **60**, 2709 (1988).
  - [17] R. H. Swendsen and J.-S. Wang, *Phys. Rev. Lett.* **58**, 86 (1987).
  - [18] L. P. Kadanoff and H. Ceva, *Phys. Rev. B* **3**, 3918 (1971).
  - [19] W. H. Press, S. A. Teukolsky, W. T. Vetterling, and B. P. Flannery, *Numerical Recipes in Fortran*, 2nd ed. (Cambridge University Press, Cambridge, 1992), Chap. 15.
  - [20] See, e.g., R. J. Baxter, *Exactly Solved Models in Statistical Mechanics* (Academic, New York, 1982).
  - [21] H. Saleur, *J. Phys. A* **20**, L1127 (1987).
  - [22] H. van Beijeren, *Phys. Rev. Lett.* **38**, 993 (1977).
  - [23] C. Itzykson and J. B. Zuber, *Nucl. Phys. B* **275**, 580 (1986).
  - [24] U. Wolff, *Phys. Rev. Lett.* **62**, 361 (1989).
  - [25] P. di Francesco, H. Saleur, and J. B. Zuber, *J. Stat. Phys.* **49**, 454 (1987).
  - [26] See M. P. Nightingale and H. W. J. Blöte, *Phys. Rev. Lett.* **76**, 4548 (1996). The value of the dynamical exponent  $z$  in this letter amounts to a two-dimensional Ising model with Glauber dynamics and random site selection. It is reasonable to suppose that any single-spin algorithm displays the same value of  $z$ .
  - [27] See, e.g., Y. M. M. Knops, B. Nienhuis, H. J. F. Knops, and H. W. J. Blöte, *Phys. Rev. B* **50**, 1061 (1994); G. Mazzeo, E. Carlon, and H. van Beijeren, *Phys. Rev. Lett.* **74**, 1391 (1995).
  - [28] A. M. Ferrenberg and R. H. Swendsen, *Phys. Rev. Lett.* **63**, 1195 (1989).